

Investigation of stress-distribution in a car tyre with regards to rolling resistance

C. Hoever, P. Sabiniarz, W. Kropp

Division of Applied Acoustics, Chalmers University of Technology,
SE 41296 Göteborg, Sweden

e-mail: carsten.hoever@chalmers.se

Abstract

In recent years the method of waveguide finite element modelling has emerged as a suitable tool for the simulation of the structural behaviour of tyres. It combines cross-sectional finite element modelling with classical wave propagation methods along the waveguide. Compared to traditional finite element methods it is numerically much more efficient and provides greater physical insights into the vibrational behaviour. In an ongoing project an existing waveguide finite element model for the calculation of stationary (non-rolling) tyre vibrations is extended to allow for calculation of the stress distributions inside a rolling tyre being in contact with the ground. The results are used to identify local areas of high stress, which are not only important from a structural point of view but which can also be associated with high energy losses due to dissipation, hence affecting the overall rolling resistance of the tyre. The procedure and preliminary results will be presented.

1 Introduction

In the year 2006 the fuel consumption in the road transportation sector was responsible for 23 % of the CO₂ emissions in the European Union [1] and 26 % in the United States [2] — in both cases with absolute emission values remaining constant or even increasing since 1990. As there is sustained demand for personal mobility and transportation services in most societies, it seems unlikely that a reduction of CO₂ emissions can be achieved by a reduction of mileage travelled. Instead, one possible way of reducing CO₂ emissions is by finding ways to increase the energy effectivity of existing means of transportation.

For cars powered by classical combustion engines, only about 10 % to 20 % of the chemical energy stored in the fuel is available as mechanical energy at the axles to drive the wheels, the remainder being consumed by engine inefficiency, friction in the driveline, standby operation or auxiliary appliances (e.g. the A/C system) [3]. Ultimately, these 10 % to 20 % are consumed by aerodynamic drag, rolling resistance and braking/acceleration. Depending on the driving conditions, approximately 4 % to 7 % of the fuel consumption are based on rolling losses in the tyres, see [3]. For trucks and other heavy vehicles, the influence is even higher [4].

Hence, a reduction of the energy losses due to rolling resistance has a strong potential of reducing a vehicle's overall fuel consumption. The Transportation Research Board of the United States, for example, has come to the conclusion that “a 10 percent reduction in average rolling resistance [...] promises a 1 to 2 percent increase in fuel economy” [3]. For the United States, this equivalent a reduction of the overall yearly fuel consumption by $3.7 \cdot 10^9$ l to $7.5 \cdot 10^9$ l.

About 80 % to 95 % percent of rolling losses can be attributed to hysteretic losses in the tyres [5], i.e. the dissipation is based on the viscoelastic properties of the tyre material. Most of the dissipation is related to

deformation of the rubber material in the tread, hence possible ways of reducing the rolling resistance are changing the tread geometry, the rubber compound or reducing the tread thickness [5]. Any change of an individual tyre parameter, however, does not only affect rolling losses, but also other important aspects like wear, traction or noise generation. This is a problem which is even intensified by the complex tyre structure with inhomogenous and anisotropic material properties. Knowledge about how the hysteretic losses are distributed in the structure of a tyre rolling on an actual road and which vibrational modes contribute mostly to these losses can help to make design decisions for tyres with a low rolling resistance.

For this, a waveguide finite element tyre model [6] is combined with a quasi three-dimensional contact model [7], to give the vibrational behaviour of the tyre when rolling on a real road. This is then used to calculate the strain energy distribution inside the tyre respectively over the different vibrational modes, which, together with the local loss factors, can be directly related to the internal damping of the tyre [8].

2 Fundamentals of rolling resistance and prediction methods

Generally, rolling resistance is defined as the mechanical energy converted into heat for a unit distance travelled [9], with a unit of J/m . Traditionally, this has been associated with a drag force of unit N opposing the direction of motion. Since the more general energy based definition seems to be more appropriate within the scope of this study, it will be used in the following. This also allows the use the term *rolling loss* as an equivalent expression for *rolling resistance*.

As mentioned before, the majority of the rolling loss can be attributed to hysteresis. During rolling, the tyre material is periodically deformed. Due to the viscoelastic properties of the rubber compound, in each cycle not all of the stored elastic energy can be regained, instead a part of it is dissipated. The main cause of deformation for a rolling tyre is the flattening of the contact patch which leads to bending of the crown, the sidewalls and the bead area, compression of the tread and shearing of the tread and the sidewall [5]. These disturbances propagate inside the tyre structure as waves in a variety of different mode shapes and orders, leading to dissipation. How dissipation is distributed among different wave modes is one of the areas of interest for this study.

For today's usually used radial tires most of the dissipation occurs in the tread which is usually made out of a rubber compound consisting of natural and/or synthetic polymers, reinforcing fillers and some additives (e.g. oils). This is due to the high loss factor of rubber and the fact that the tread is comparably soft (especially when compared to the belt with its reinforcing plies), allowing for large deformations and hence a high potential energy.

The viscoelastic properties of the rubber compound are highly temperature and frequency dependent [10]. Additionally, the rolling resistance shows a more or less prominent dependence on a variety of features such as tyre load, tyre geometry, tyre pressure, driving speed, (road) surface geometry, condition and roughness, etc. A thorough description of these effects is outside the scope of this study, detailed information can for example be found in [4, 5].

In this study, the main focus will be on developing a method which is suitable for the evaluation of the distribution of potential energy inside a rolling tyre. Moreover, the influence of vibrational parameters like frequency and mode order is investigated. For this, the aforementioned parameters are kept fixed in this study. At later stages the model will be used to evaluate the dependence of rolling resistance on changes in certain parameters such as a type of tyre or road.

The method is based on the property that the energy dissipation within a structure is determined by the product between local potential energy and local loss factors [8], hence potential energy and rolling loss are directly related. At this stage, the method does not aim at calculating detailed values for the dissipated energy. This is due to the fact that this would require full knowledge about the loss factor in specific regions of the tyre, which is not available in the necessary detail level. Even though basically every tyre model includes some assumptions on loss factor characteristics for the tyre, these values vary considerably between

different models¹ and it is believed that good simulation results for certain cases (such as point and transfer mobility calculations) do not automatically indicate exact loss factor assumptions, especially not on a more local level. A notable effort at estimating viscoelastic details for a tyre structure is made in [11], however the employed process is quite tedious and requires dedicated measurements of the specific tyre. Hence, dissipation will be assumed to be based on a set of rather global loss factor assumptions for the time being.

A good summary of existing literature on the evaluation of rolling losses can be found in [3]. For the sake of brevity, only a few models are mentioned in the following. Both Hall and Moreland [4] and Lin and Hwang [12] calculate the dissipation based heat distributions inside a rolling tyre. References to tyre vibrations are, however, not drawn. Yam et al. [13] base their work on experimental modal analysis data, leading to total values for rolling resistance based on different velocities or loads. Stutts and Soedel [14] use a stationary tension band on an elastic foundation to calculate the rolling resistance from the deflection in the contact zone. The work of Fraggstedt [11] is the basis for this analysis. He calculates the dissipated power inside a tyre based on the imaginary parts of the stiffness and mass matrices of a waveguide finite element model of a tyre rolling on a road. Frequency and wave order distributions are shown as well as individual element contributions to the overall dissipation. However, a detailed analysis of the results is missing, instead the focus is on the calculation of total dissipated power for individual road surfaces. Also, this approach relies heavily on an accurate loss factor data for the definition the complex stiffness and mass matrices.

2.1 Review of existing tyre models

Since the mid-1960s, a variety of different models have been developed, aiming at simulating the dynamic response of tyres. They range from analytical models, based on coarse simplifications of the geometrical and material properties, to highly sophisticated numerical models, accounting for the detailed physical properties of tyres. In the following, a selection of tyre models found in the open scientific literature is reviewed.

One of the first models was presented by Böhm in [15], where the tyre belt was described as a pretensioned ring, resting on a Winkler bedding. The bedding represents the sidewalls and the enclosed air cavity, whereas the pretension force is due to the inflation pressure. The general idea of modelling the vibrational behaviour as some kind of ring or plate structure on an elastic foundation has thereafter been used in many more and more refined variations, e.g. by Kropp and co-workers [16, 17, 18], Kim and Bolton [19], Muggleton et al. [20] or more recently by Kindt et al. [21]. Although these models are simple, fast and generally capture the dynamic behaviour quite well within a certain frequency region, they are of limited use when the local stress distribution is of interest, as they lack the necessary level of structural detail.

The rapid development of computer capacity during recent decades has made it possible to perform detailed modelling of tyres using the finite element method (FEM). A number of examples are found in the literature, of which a few are Kung et al. [22], Richards [23] and Pietrzyk [24], who all modelled free or forced response cases. The response of rotating tyres, making contact with the ground, was modelled by Fadavi et al. [25], Brinkmeier et al. [26] and by Lopez et al. [27]. Generally, FEM models, although flexible and capable of giving insight into local properties, suffer from high requirements on computer capacity and need for detailed input data.

Waki et al. [28] presented a model based on an approach in which the tyre is considered as a waveguide along the circumferential direction. Initially, a short section of the waveguide is modelled using standard finite elements. A periodicity condition is then applied. This results in an eigenvalue problem from which the dispersion properties and cross-section modes are obtained. Nilsson [29] developed a model based on the waveguide finite element method (WFEM). This approach is related to that of Waki et al. in the sense that it also makes use of an FE technique to model the response of waveguides. The model considers the structural as well as fluid domain, using waveguide finite elements of the thin shell type, fluid type and fluid–structure coupling type. A modified version of the model in [29] has also been presented in [11], where thick shell

¹A short literature study revealed that loss factors used for the belt region vary from 0.04 to 0.25 between different publications.

elements were used to model the sidewalls and belt and solid elements to model the tread. An additional difference as compared to [29] is that the air cavity was excluded. By utilising the waveguide properties of the tyre, the computational burden is significantly reduced compared to traditional FEM modelling. Also the wave characteristics are more directly captured than with the FEM.

The model described in [11], with one simplification introduced, has also been implemented by two of the authors to describe the wave field in a stationary tyre (cf. [6]). The model is also well suited for the assessment of rolling losses as intended here: Hamilton's principle, which is used for the derivation of the governing equations, inherently includes a description of the potential energy and due to being an assembly of individual elements, the investigation is easily possible on a sub-structure basis. Some details of the model will be described in the Sec. 3.1.

3 The tyre model

3.1 Waveguide finite element modelling

The waveguide finite element model of the tyre being used in this study is, apart from some small changes, identical to the one previously described by two of the authors in [6]. It is modified version of the model presented in Paper B of [11] with differences being the omission of the rim from the assembly and changes in the implementation of damping. In the following a short overview of waveguide finite element modelling is given.

A waveguide is a system which has constant geometrical and material properties along one, typically "long" dimension, along which the motion can be described conveniently by a set of propagating waves with the right set of boundary conditions. In this sense a tyre is a waveguide for which the motion along the circumferential dimension can be described by a set of waves fulfilling a periodicity condition $\mathbf{u}(\phi) = \mathbf{u}(\phi \pm 2\pi)$, where \mathbf{u} denotes the tyre displacement.

Typical other waveguide examples include beams and plates [31] or rails [32]. In the waveguide finite element method (WFEM) the waveguide property is used in conjunction with conventional two-dimensional finite element modelling of the waveguide cross-section, i.e. in a cylindrical coordinate system the displacement component u_i for a point (r, x, ϕ) is given by (time dependency $e^{j\omega t}$ dropped in the following)

$$u_i(r, x, \phi) = \mathbf{N}(r, x)\mathbf{v}_i(\phi) \quad i = r, x, \phi. \quad (1)$$

Herein, \mathbf{N} is a vector of cross-sectional FE shape functions while \mathbf{v}_i represents the corresponding nodal degrees of freedom. Thus, only the displacement dependance on the cross-sectional coordinates is approximated using FE modelling, while the nodal displacements are functions of the angular coordinate ϕ . Hence, they depend on the assumed wave propagation along this dimension.

Finnveden and Fraggstedt have shown [30] that based on Eq. (1), using a modified Hamilton's principle which accounts for harmonic response and the viscoelastic properties of the tyre material, and application of common FE procedures, a set of coupled ordinary differential equations is obtained:

$$\left[-\mathbf{A}_{11} \frac{\partial^2}{\partial \phi^2} + (\mathbf{A}_{01} - \mathbf{A}_{10}) \frac{\partial}{\partial \phi} + \mathbf{A}_{00} - \omega^2 \mathbf{M} \right] \mathbf{v}(\phi) = \mathbf{f}(\phi). \quad (2)$$

The generalised stiffness matrices \mathbf{A}_{nm} and the mass matrix \mathbf{M} are derived from the tyre's potential respectively kinetic energies and \mathbf{f} is the generalised force vector describing the external load. By setting $\mathbf{f} = 0$ the homogeneous case is obtained, for which solutions are given by exponential functions of kind

$$\mathbf{v}(\phi) = \hat{\mathbf{v}} e^{i\kappa\phi}. \quad (3)$$

These can be physically interpreted as waves of cross-sectional mode shape \hat{v} travelling along the circumferential direction with polar wavenumber κ . Inserting (3) into (2) results in an eigenvalue problem which can be solved to get the eigenfrequencies and mode shapes for a specific polar wave number. The forced response case, (i.e. the solution to the inhomogeneous form of (2)), can for example be solved by means of an assumed mode procedure as described in [11].

3.2 Modelling of rolling contact

The model for the contact between the rolling tyre and the road surface is based on quasi-3D model described in [7]. It accounts for the radial contact forces which are due to the indenting of the road roughness into the tyre tread. To get accurate results, three-dimensional roughness data is necessary, i.e. it is not sufficient to include only one roughness track along the circumferential direction, it has also to be accounted for the roughness variation along the lateral direction. It has also to be considered that the tyre vibrations are a function of the contact forces while, at the same time, the contact forces also are a function of the tyre vibrations. This non-linearity leads to a formulation in the time domain.

For a specific contact patch and radial contact forces, the dynamic problem can be described by the following system of equations

$$\mathbf{F}(t) = \mathbf{C}^{-1} \Delta \mathbf{y}(t) \quad (4a)$$

$$\Delta \mathbf{y}(t) = y_0(t) + \mathbf{k}_r(t) + \boldsymbol{\xi}(t) - \mathbf{k}_t(t) \quad (4b)$$

$$\xi_n(t) = \sum_m F_m(t) * g_{m,n}(t), \quad (4c)$$

where $\mathbf{F}(t)$ are the contact forces for all contact points, \mathbf{C} is an influence matrix obtained from an elastic-half space representation of the tyre tread and $\Delta \mathbf{y}(t)$ is the deformation of the tread. $y_0(t)$ denotes the centre position of the rim whereas $\mathbf{k}_r(t)$ and $\mathbf{k}_t(t)$ describe the profile of the road roughness and the tyre and are obtained from scanning of the actual surfaces. Finally, $\boldsymbol{\xi}(t)$ is the dynamic displacement of the tyre structure around the neutral line. Its components $\xi_n(t)$ are given by the convolution of the contact force $F_m(t)$ at position m , with the Green's function $g_{m,n}(t)$. The Green's functions can be directly obtained from the WFE model described in Sec. 3.1 by calculation the responses for point force excitation and subsequent Fourier transformation. The set of equations (4) is finally iteratively solved for every time step.

In order to decrease the computational burden and due to the nature of the WFEM mesh, different levels of discretisation are used for the road roughness and tyre profiles. Whereas the discretisation of the road and tyre profiles is very fine to capture even small variations, the discretisation of the contact patches on the tyre structure is coarser, i.e. the contact forces are integrated locally to excite specific solid elements of the tread structure. The validity of this approach is shown in [7]. By transformation to the frequency domain and adaption to the WFEM tyre model, the generalised force $\mathbf{f}(\phi)$ in Eq. (2) is obtained from $\mathbf{F}(t)$.

3.3 Strain energy and power dissipation

According to [30] the strain potential for a viscoelastic material is given as

$$\bar{U} = \int_V \boldsymbol{\epsilon}^{aT} \mathbf{D} \boldsymbol{\epsilon} dV \quad (5a)$$

$$= \int_0^{2\pi} \sum_{n=0}^1 \sum_{m=0}^1 \frac{\partial^n \mathbf{v}^{aT}}{\partial \phi^n} \mathbf{A}_{nm} \frac{\partial^m \mathbf{v}}{\partial \phi^m} d\phi \quad (5b)$$

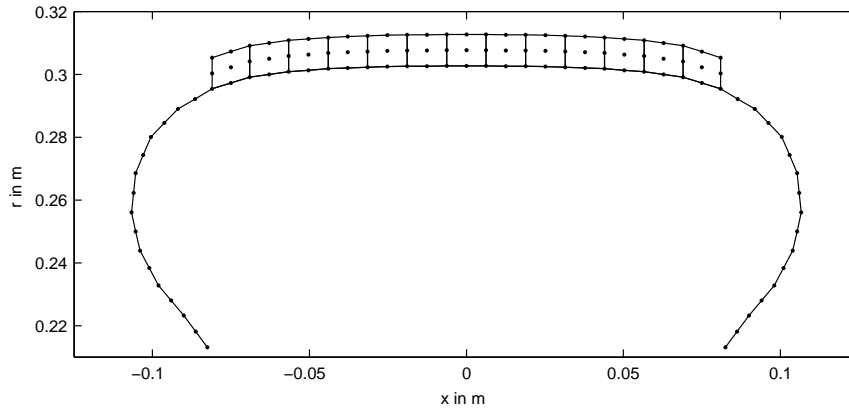


Figure 1: Mesh of the modelled 205/55R16 tyre. Each \bullet represents one node with each shell element having three and each solid element having nine nodes.

Eq. (5a) gives the general strain potential relation for the domain V , based on the engineering strain ϵ and the rigidity matrix \mathbf{D} , while Eq. (5b) follows from the application of the WFEM principle (1), the strain-displacement relations and the assembly of the cross-section structure. T denotes transpose and a denotes the complex conjugate in an mathematically adjoint system with negative damping. The latter is a conceptual trick used in the formulation of the variational principle for viscoelastic materials upon which Eq. (2) is based. For details the reader is referred to [30].

Since the stiffness matrices \mathbf{A}_{nm} are based on the FE element formulations and the subsequent assembly process, it is possible to calculate the strain potential \hat{U} for individual elements, the whole tyre or any sub-structure in-between, as long as the nodal displacements v are known. Upon this basis a detailed investigation of the strain potential distribution in the tyre structure is possible. From this, an evaluation of the dissipated power can be conducted.

3.4 Modelling details

In this study a model similar to that of the 205/55R16 tyre as previously described in [6] is used. It consists of 29 deep shell elements which constitute the sidewalls and the belt, and 13 two-dimensional solid elements which are used to model the rubber tread. In [11] a mesh of similar size is shown to give sufficient results up to at least 1000 Hz, which was also proven by a small convergence study. Along the tyre circumference, 512 response positions are evaluated.

The deep shell elements account for anisotropy, rotational inertia, shearing across the element and pretension due to the tyre inflation and are based on quadratic shape functions. The solid elements are of isotropic, two-dimensional Lagrange type. A detailed description of both element types can be found in [30]. The resulting cross-sectional tyre mesh can be found in Fig. 1. Even though a complete tyre has a very complicated internal structure, this mesh is sufficient for a waveguide finite element model since, neglecting the tread pattern, the cross-sectional geometry and material parameters are constant along the circumferential direction.

As previously mentioned, the tyre is considered not to have any tread groves. Moreover, the air cavity is not explicitly modelled (but the resulting pre-tension is included) as fluid and structure modes are only weakly coupled in tyres [23]. Hence, it is believed that the influence of the cavity modes on the stress distribution can be neglected. Also the wheel is not included in the simulations since its influence is mostly relevant when comparing low frequency response between simulations and measurements on a freely suspended tyre where the rim's mass considerably influences the low frequency behaviour. Concluding, it is believed that it is sufficiently to simulate the influence of the wheel by blocking the tyre motion at the bead and the influence of the air cavity by including pre-tension due to inflation in the shell elements.

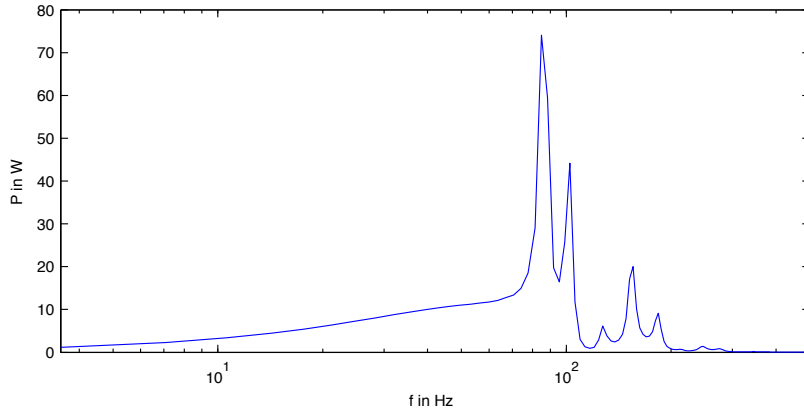


Figure 2: Dissipated power as function of frequency. Frequencies higher than 500 Hz omitted due to negligible influence on dissipation.

Most of the required input data for the elastic properties, pretension forces, densities and damping parameters is based on an input deck provided by a tyre manufacturer and a subsequent refinement of this data based on a comparison of simulation results to measured transfer functions. In the following a brief overview of the input parameters is given, for a detailed description of this process see [6].

For the isotropic solid elements in the tread a frequency independent Young's modulus E of roughly 20 MPa and a Poisson's ratio ν of 0.49 are assumed. The necessary stiffnesses for the shell elements are directly taken from the input deck, with the following small adaptations: A small frequency dependance included in the input deck data is neglected, missing values for shear stiffnesses across the element thickness are set to be equal to the in-plane shear stiffness and the circumferential bending stiffness is reduced by 50 %. Adaption of the pretension values includes a correction of unphysical lateral pretension near the beds and a reduction of the circumferential pretension by 25 %.

Damping is based on a stiffness-proportional model. For the shell elements the frequency dependent loss factor η assumes a value of 0.05 below the cut-on frequency of the first symmetric belt bending mode and 0.15 above it with a transition region extending from roughly 280 Hz to 370 Hz. For the solid elements representing the highly damped rubber, the loss factor is set to $\eta = 0.25$.

For the rolling contact a speed of 50 km/h and a loading of 3000 N are assumed. The tyre surface profile is taken from a measurement of a slick tyre profile and the road roughness profile is based on a scan of 15 lateral tracks of an drum-mounted ISO 512 road surface. Rolling losses are averaged over a road surface length corresponding to three full tyre revolutions. The obtained frequency resolution is 3.5 Hz.

4 Results

Due to time constraints only preliminary results are shown in the following. Figures 2 and 3 show the distribution of the dissipated power over frequency respectively circumferential wave order. All of the relevant dissipation occurs below 200 Hz, with a considerable level of dissipation in a broad low frequency region, followed by a very distinct maxima at 85 Hz and two other maxima of lesser importance at 103 Hz and 154 Hz. In the circumferential wave order domain, dissipation is concentrated at wave orders 1 to 5 with an emphasis on orders 1, 2 and, to a lesser degree, 4. Wave orders 10 and higher only contribute to a very small extent to the dissipation.

Additional insight into the distribution of the rolling losses between different frequencies and wave orders can be gained by Fig. 4. Therein, a majority of the dissipation occurring at 85 Hz can be related to wave order 1. According to [6] this corresponds to a semi-rigid body mode of the tyre where the belt acts as a rigid ring being displaced in radial direction as shown in Fig. 5. Similar relations can be established between the

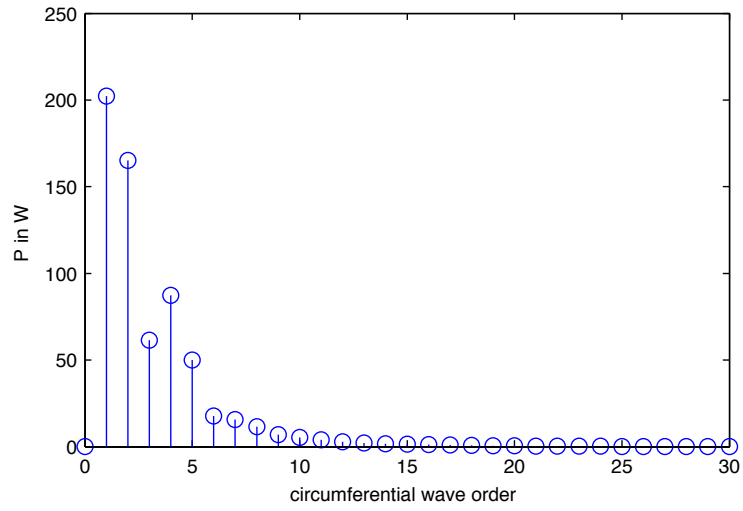


Figure 3: Dissipated power as a function of circumferential wave order.

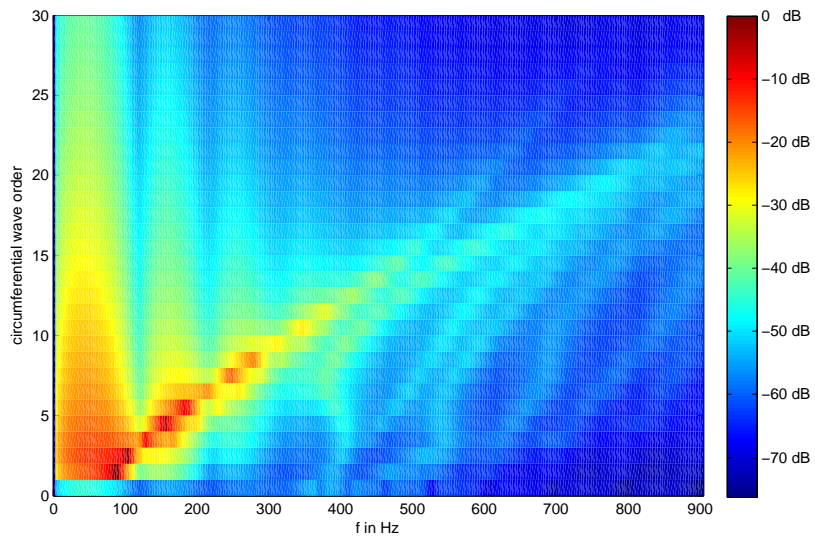


Figure 4: Dissipated power as a function of frequency and circumferential wave order. Colour scaling is in dB re. maximum of plot.

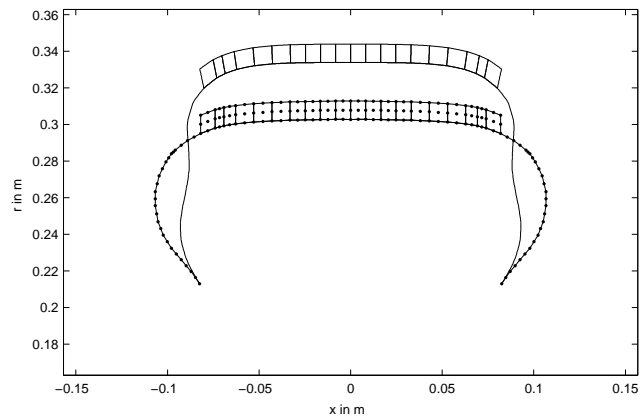


Figure 5: Cross-sectional mode shape for 85 Hz and wave order 1. Note: Shown mesh is not the one used in this study.

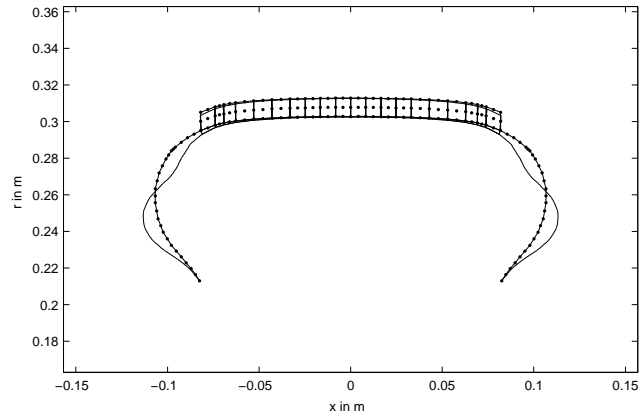


Figure 6: Cross-sectional mode shape for 625 Hz and wave order 20. Note: Shown mesh is not the one used in this study.

dissipation peaks at 103 Hz respectively 154 Hz and circumferential wave orders 2 respectively 4. In both cases the cross-sectional mode shape is basically identical to the one previously shown for the semi-rigid case, i.e. it is dominated by a radial motion of the whole tread region as shown in Fig. 4. Accordingly, all three modes are strongly excited by radial forces applied to the tread. An analysis of dispersion relations conducted in [6] reveals that all three cases belong to a set of waves with similar cross-sectional shapes. The concentration of rolling losses along a nearly straight line up to wave order 15 at approximately 500 Hz in Fig. 4 can also be attributed to this wave set. The importance of these waves for the rolling resistance decreases with increasing frequency, which is due to a gradual change of cross sectional mode shape towards higher frequencies, until there is no tread deformation anymore and only side-wall motion, see Fig. 6. In addition, with increasing order the wavelength becomes equal or smaller than the contact length (which is around 10 cm), which means that the contribution of these modes to the global deformation of the tyre structure in the contact area is rapidly decreasing. This might explain the change in Fig. 4 from order 9 to order 10. For order 9, the circumferential wavelength is about twice the contact length. Still, below wave order 11 and 400 Hz major parts of the dissipation can clearly be associated with this set of waves.

In Fig. 4 further sets of waves can be identified, all of which represent symmetric belt bending modes which are characterised by an odd number M of half wavelengths of out-of-plane displacement over the cross

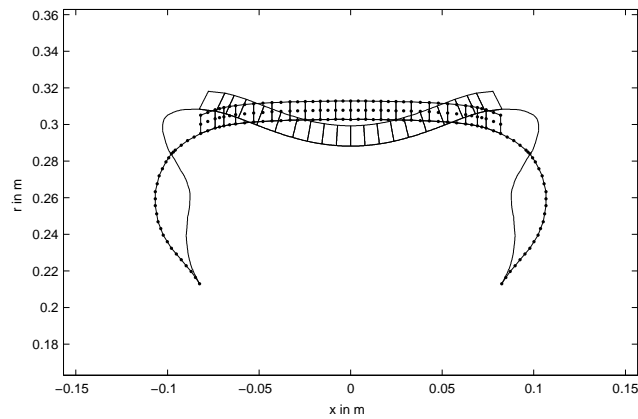


Figure 7: Cross-sectional mode shape for 385 Hz and wave order 8. Note: Shown mesh is not the one used in this study.

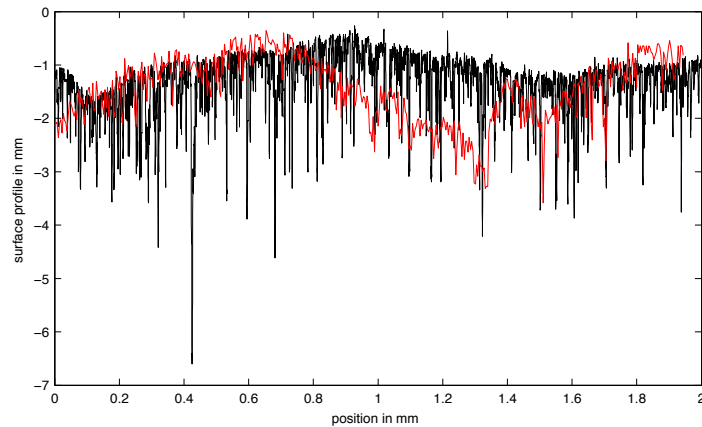


Figure 8: Comparison of used drum-mounted ISO road surface profile (red) with typical ISO surface profile (black).

section, as shown exemplarily for $M = 5$ in Fig. 7. Their overall contribution to the dissipation, however, is of minor importance.

Contrary to this concentration of dissipation to individual wave orders for frequencies above approximately 80 Hz, a more widespread distribution of rolling losses can be found in the lower frequency regime, covering wave orders from 1 to 15 or even higher. This might be caused by the low frequency nature of the contact excitation and the lack of tyre eigenmodes in this region. Due to the characteristics of the specific ISO road profile scan, a strong low frequency content is inherent in the excitation, see Fig. 8 where a part of the used, drum-mounted, ISO road surface scan is compared to a typical ISO surface.

The local distribution of power dissipation between the different elements can be seen in Fig. 9. The lack of symmetry can be explained by the specific characteristics of the ISO road surface where a higher road profile can be found for one side. The fact that most dissipation occurs in the shell elements is somewhat unexpected but might be related to the specific tyre investigated in this study.

Finally, the total dissipated power is given as 643 W, a value which is in the same range as expected from the results shown in [11].

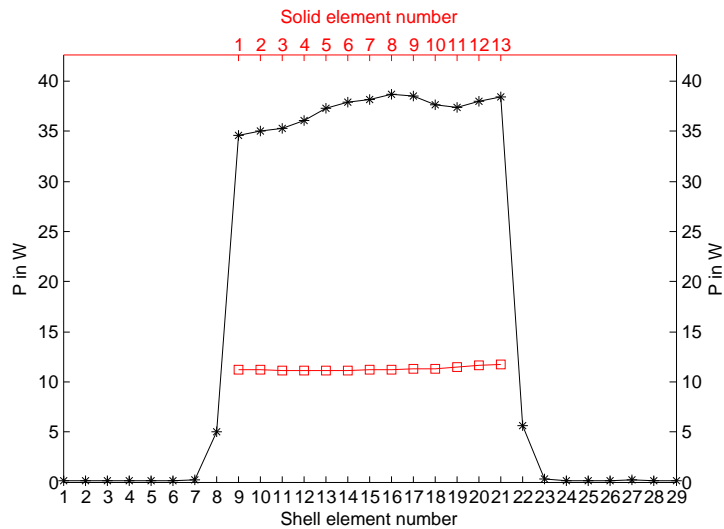


Figure 9: Distribution of dissipation between individual shell (black *) and solid (red □) elements. Asymmetry due to local features of the road roughness profile.

5 Conclusion

A way is shown how to assess rolling losses based on the strain energy distribution in an existing waveguide finite element model of a car tyre which is coupled with a quasi three-dimensional model for rolling contact. Preliminary results based on a specific ISO road roughness profile are used to show the general applicability of this approach. The estimated total rolling loss is comparable to values found in the literature and detailed examination of the frequency and wave order content reveal the importance of the contact patch size and a strong influence of a limited set of tyre modes on the rolling resistance. In general, rolling resistance seems to be a low-frequency, low wave order problem. The solid rubber elements seem to contribute less to the dissipation as expected, which will be the topic of further investigations in the future. A necessary improvement is an averaging over a longer section of road roughness profiles to reduce the influence of very specific local characteristics. This was only partly possible for this study due to time constraints. Further studies will include evaluation of the influence of different conditions such as road profile, speed, loading, etc. on the rolling loss distribution.

Acknowledgements

The work presented in this paper has been financially supported by the European Commission research project *Green City Car*, SCP8-GA-2009-233764.

References

- [1] *Annual European Community greenhouse gas inventory 1990–2006 and inventory report 2008*, Technical report No 6/2008, European Commission, European Environment Agency (2008).
- [2] *Inventory of U.S. greenhouse gas emissions and sinks: 1990 – 2008*, Technical Report EPA 430-R-10-006, U.S. Environmental Protection Agency (2010).

- [3] *Tires and passenger vehicle fuel economy: Informing consumers, improving performance*, Technical Report 286, Committee for the National Tire Efficiency Study, Transportation Research Board, Board on Energy and Environmental Systems (2006).
- [4] D. Hall, J. Moreland, *Fundamentals of rolling resistance*, Rubber Chemistry and Technology, Vol. 74, No. 3, Rubber Division ACS (2001), pp. 525–539.
- [5] A. Gent, J. Walter, editors, *The pneumatic tire*, U.S. Department of Transportation, National Highway Traffic Safety Administration (2006).
- [6] P. Sabiniaz, W. Kropp, *A waveguide finite element aided analysis of the wave field on a stationary tyre, not in contact with the ground*, Journal of Sound and Vibration, Vol. 329, No. 15, Elsevier (2010), pp. 3041–3064.
- [7] F. Wullens, *Excitation of tyre vibrations due to tyre/road interaction*, PhD thesis, Chalmers University of Technology, Göteborg (2004).
- [8] G. Pavic, *The role of damping on energy and power in vibrating systems*, Journal of Sound and Vibration, Vol. 281, No. 1-2, Elsevier (2005), pp. 45–71.
- [9] *ISO 18164 passenger car, truck, bus and motorcycle tyres — methods of measuring rolling resistance*, International Organization for Standardization (2005).
- [10] A. Nashif, D. Jones, J. Henderson, *Vibration damping*, Wiley-Interscience (1985).
- [11] M. Fraggstedt, *Vibrations, damping and power dissipation in car tyres*, Phd thesis, Royal Institute of Sciences, Stockholm (2008).
- [12] Y. Lin, S. Hwang, *Temperature prediction of rolling tires by computer simulation* Mathematics and Computers in Simulation, Vol. 67, No. 3, Elsevier (2004), pp. 235–249.
- [13] L. Yam, J. Shang, D. Guan, A. Zhang, *Study on tyre rolling resistance using experimental modal analysis*, International Journal of Vehicle Design, Vol. 30, No. 3, Inderscience (2002), pp. 251–262.
- [14] D. Stutts, W. Soedel, *A simplified dynamic model of the effect of internal damping on the rolling resistance in pneumatic tires*, Journal of Sound and Vibration, Vol. 155, no. 1, Elsevier (1992), pp. 153–164.
- [15] F. Böhm, *Mechanik des Gürtelreifens* Archive of Applied Mechanics, Vol. 35, No. 2, Springer (1966), pp. 82–101.
- [16] W. Kropp, *Structure-borne sound on a smooth tyre*, Applied Acoustics, Vol. 26, No. 3, Elsevier (1989), pp. 181–192.
- [17] W. Kropp, *Ein Modell zur Beschreibung des Rollgeräusches eines unprofilierten Gürtelreifens auf rauher Straßenoberfläche*, Fortschrittberichte VDI, Reihe 11: Schwingungstechnik, No 166, VDI Verlag (1992).
- [18] K. Larsson, W. Kropp, *A high-frequency three-dimensional tyre model based on two coupled elastic layers*, Journal of Sound and Vibration, Vol. 253, No. 4, Elsevier (2002), pp. 889–908.
- [19] Y. Kim, J. Bolton, *Modelling tyre treadband vibration*, in R. Boone, editor, *Proceedings of The 2001 International Congress and Exhibition on Noise Control Engineering, The Hague, The Netherlands, 2001 August 27-30*, The Hague (2001).
- [20] J. M. Muggleton, B. R. Mace, M. J. Brennan, *Vibrational response prediction of a pneumatic tyre using an orthotropic two-plate wave model*, Journal of Sound and Vibration, Vol. 264, No. 4, Elsevier (2003), pp. 929–950.

- [21] P. Kindt, P. Sas, W. Desmet, *Development and validation of a three-dimensional ring-based structural tyre model*, Journal of Sound and Vibration, Vol. 326, No. 3–5, Elsevier (2009), pp. 852–869.
- [22] L. Kung, W. Soedel, T. Yang, *Free vibration of a pneumatic tire-wheel unit using a ring on an elastic foundation and a finite element model*, Journal of Sound and Vibration, Vol. 107, No. 2, Elsevier (1986), pp. 181–194.
- [23] T. Richards, *Finite element analysis of structural-acoustic coupling in tyres*, Journal of Sound and Vibration, Vol. 149, No. 2, Elsevier (1991), pp. 235–243.
- [24] A. Pietrzyk, *Prediction of the dynamic response of a tyre*, in R. Boone, editor, *Proceedings of The 2001 International Congress and Exhibition on Noise Control Engineering, The Hague, The Netherlands, 2001 August 27-30*, The Hague (2001).
- [25] A. Fadavi, D. Duhamel, H. Yin, *Tyre/road noise: Finite element modelling of tyre vibrations*, in R. Boone, editor, *Proceedings of The 2001 International Congress and Exhibition on Noise Control Engineering, The Hague, The Netherlands, 2001 August 27-30*, The Hague (2001).
- [26] M. Brinkmeier, U. Nackenhorst, S. Petersen, O. von Estorff, *A finite element approach for the simulation of tire rolling noise*, Journal of Sound and Vibration, Vol. 309, No. 1–2, Elsevier (2008), pp. 20–39.
- [27] I. Lopez, R. Blom, N. Roozen, H. Nijmeijer, *Modelling vibrations on deformed rolling tyres—a modal approach*, Journal of Sound and Vibration, Vol. 307, No. 3–5, Elsevier (2007), pp. 481–494.
- [28] Y. Waki, B. Mace, M. Brennan, *Free and forced vibrations of a tyre using a wave/finite element approach*, Journal of Sound and Vibration, Vol. 323, No. 3–5, Elsevier (2009), pp. 737–756.
- [29] C.-M. Nilsson, *Waveguide finite elements applied on a car tyre*, PhD thesis, Royal Institute of Sciences, Stockholm (2004).
- [30] S. Finnveden, M. Fraggstedt, *Waveguide finite elements for curved structures*, Journal of Sound and Vibration, Vol. 312, No. 4–5, Elsevier (2008), pp. 644–671.
- [31] D. Duhamel, B. Mace, M. Brennan, *Finite element analysis of the vibrations of waveguides and periodic structures*, Journal of Sound and Vibration, Vol. 294, No. 1–2, Elsevier (2006), pp. 205–220.
- [32] L. Gavric, *Computation of propagative waves in free rail using a finite element technique*, Journal of Sound and Vibration, Vol. 185, No. 3, Elsevier (1995), pp. 531–543.